Supporting Information

$Ti_3C_2T_X$/Graphene Aerogels for High-Efficiency Hydrovoltaic Power Generation: Performance Optimization and Mechanism Elucidation

Tianran Zhao[a†], Sai Li[b†], Yi'na Yang[a], Liyang Zhao[a], Jia Chen[a], Chunna Yu[c], Chang Zhao[c], Guangjian Xing[a*]

a College of New Materials and Chemical Engineering, Beijing Institute of Petrochemical Technology, Beijing 102617, China

b China Building Materials Academy, Beijing 100024, China

c Zhiyuan School of Liberal Arts, Beijing Institute of Petrochemical Technology, Beijing 102617, China

† Tianran Zhao and Sai Li contributed equally to this work.

* Corresponding author. E-mail address: xingguangjian@bipt.edu.cn.

S1. Adsorption Experiments and Mechanism

In the adsorption experiments, 5 mg of TGAs was immersed in 20 mL of the dye solutions with different concentrations. To minimize experimental error, parallel experiments were performed in triplicate. For cyclic adsorption experiments, TGAs was washed with ethanol to remove adsorbed dyes, before proceeding to the next adsorption cycle. The concentration of the dye solutions was quantitatively analyzed via measuring their absorbance at respective characteristic maximum wavelengths using a UV-visible spectrophotometer (UV-2600, Shimadzu). The adsorption capacity (q_t) was calculated using the following equation [1]:

$$q_t = \frac{C_i \times V - C_t \times V}{W} \quad (1)$$

where C_i (mg L^{-1}) stands for the initial concentration of the dye solution, C_t (mg L^{-1}) denotes the concentration at the adsorption time t (min), V (L) is the solution volume, and W (g) is the mass of TGAs used.

The pseudo-first-order and pseudo-second-order kinetic models were employed to elucidate the adsorption mechanism of TGAs. The models are described as follows [1]:

Pseudo-first-order:

$$\ln\left(q_e - q_t\right) = lnq_e - k_1 t \quad (2)$$

Pseudo-second-order:

$$\frac{t}{q_t} = \frac{t}{q_e} + \frac{1}{k_2 q_e^2} \quad (3)$$

where q_e (mg g^{-1}) denotes the adsorption capacity of $Ti_3C_2T_X$/GAs for the dye/drug at adsorption equilibrium, k_1 (min^{-1}) and k_2 (g mg^{-1} min^{-1}) represent the pseudo-first-order and pseudo-second-order adsorption rate constants, respectively.

To elucidate the adsorption mechanism, kinetic studies were conducted for the CR and MB adsorption process on TGA-1/2. Linear fittings were performed using pseudo-first-order and pseudo-second-order kinetic models, with the results displayed in Fig. S1. The corresponding kinetic parameters are summarized in Table S1. The calculated equilibrium adsorption capacities ($q_{e(cal)}$) for CR dye derived from the pseudo-first-order and pseudo-second-order models are 147.3 mg g^{-1} and 291.5 mg g^{-1}, with correlation coefficients (R^2) of 0.85 and 0.99, respectively. Notably, the $q_{e(cal)}$ value from the pseudo-first-order model deviates substantially from the experimental q_e, indicating a significant discrepancy. In contrast, the pseudo-second-order model yields a $q_{e(cal)}$ that is in excellent agreement with the experimental value. Furthermore, the results of kinetic analyses of MB adsorption on TGA-1/2 further confirm that the adsorption mechanism follows the pseudo-second-order model: the $q_{e(cal)}$ values are 117.4 mg g^{-1} (pseudo-first-order, R^2=0.93) and 230.4 mg g^{-1} (pseudo-second-order, R^2=0.99).

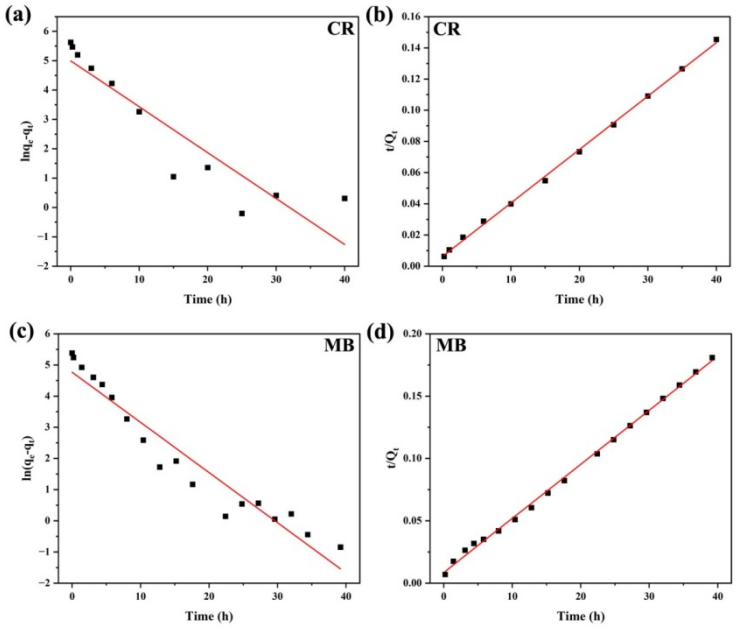

Fig. S1. (a) pseudo-first-order linear fitting model and (b) pseudo-second-order nonlinear fitting model for the adsorption of CR by TGA-1/2, (c) pseudo-first-order linear fitting model and (d) pseudo-second-order nonlinear

fitting model for the adsorption of MB by TGA-1/2.

Table S1. The parameters of adsorption model for CR and MB with TGA-1/2.

Dye	Pseudo-first-order model			Pseudo-second-order model		
	$q_{e(cal)}$ (mg g^{-1})	k_1 (min^{-1})	R_1^2	$q_{e(cal)}$ (mg g^{-1})	$k_2\times10^{-3}$ (g mg^{-1} min^{-1})	R_2^2
CR	147.3	0.16	0.8517	291.5	1.39	0.9989
MB	117.4	0.16	0.9342	230.4	2.20	0.9981

S2. Cyclic Adsorption Capabilities

To further assess its practical applicability, the cyclic stability of TGAs was investigated through multiple adsorption-desorption cycles. As illustrated in Fig. S2, the equilibrium adsorption capacities of TGA-1/2 for CR dyes over 5 consecutive cycles exhibit minimal fluctuations while maintaining remarkable consistency. Specifically, the adsorption capacity for CR is 276.6 mg g^{-1} in the first cycle, and only shows a slight decrease with the increase of cycle times, retaining 95.6% of the initial adsorption capacity after 5 consecutive cycles (adsorption capacity: 264.5 mg g^{-1}).

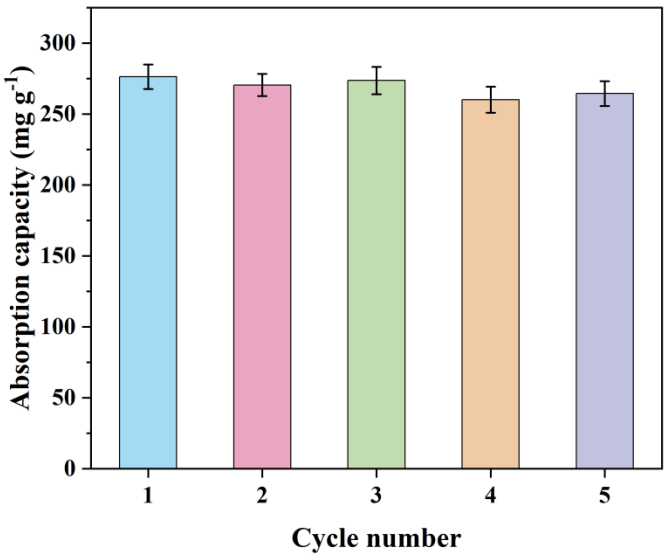

Fig. S2. Cyclic adsorption performance of TGA-1/2 toward CR dye.

Table S2 presents a comparative analysis of the adsorption capacities of TGAs against various reported adsorbents for organic pollutants. It is evident that the adsorption performance of TGAs toward dyes is either comparable to or significantly superior to the values documented in the literature, thereby confirming its great potential as a high-performance adsorbent for environmental remediation.

Table S2. Comparison of adsorption capacity of different adsorbents for organic pollutants.

Adsorbent	Dye	q_e (mg g^{-1})	Ref.
Alkali treated $Ti_3C_2T_X$	MB	189	2
$Ti_3C_2T_X$	MB	~140	3
PVA/GA	MB, RhB	88, 139	4
$Ti_3C_2T_X$/carbon foam	MB	356.97	5
Graphene oxide	MB, BPB	179.21, 236.42	6

Nanosheets/chitosan aerogel			
Feather keratin/silk fibroin aerogels	MB	163.84	7
Nanocellulose/gelatin biomass aerogel	MB, CR	182.6, 590.6	8
Chitosan/sodium alginate aerogels	MB	59.6	9
Palygorskite-based aerogel	MB	~45	10
Polyethyleneimine-modified sodiumalginate/carboxylated chitosan/attapulgite aerogels	MB, CR	206, 290.13	11
Amino-functionalized graphene aerogels	MB, GV, SF-T, MO, RB-5	281.8−370.5, 51.61−125.7	12
TGAs	CR, MB	276.6, 217.2	This work

S3. Zeta Potential

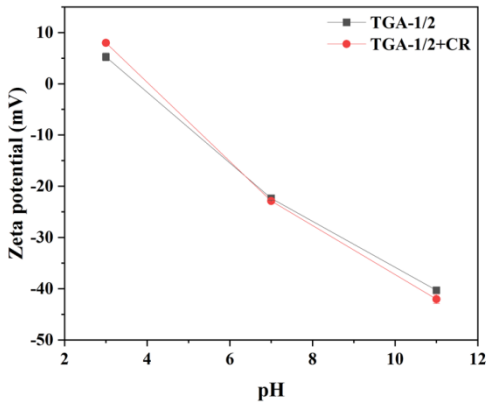

Fig. S3. Zeta potential of TGA-1/2 before and after CR adsorption.

References

[1] M. Liu, H. Pu and D.W. Sun, *Carbohyd. Polym*., 2025, **357**, 123410.

[2] W. Zheng, P. Zhang, W. Tian, X. Qin, Y. Zhang and Z. Sun, *Mater. Chem. Phys.*, 2018, **206**, 270–276.

[3] B.M. Jun, J. Heo, N. Taheri-Qazvini, C.M. Park and Y. Yoon, *Ceram. Int.,* 2020, **46**, 2960–2968.

[4] S. Tang, D. Xia, Y. Yao, T. Chen, J. Sun, Y. Yin, W. Shen and Y. Peng, *J. Colloid. Interf. Sci*., 2019, **554**, 682–691.

[5] X. Wang, Q. Xu, L. Zhang, L. Pei, H. Xue and Z. Li, *J. Environ. Chem. Eng*., 2023, **11**, 109206.

[6] Y. Li, H. Liu, R. Nie, Y. Li, Q. Li, Y. Lei, M. Guo and Y. Zhang, *Ind. Crop. Prod.*, 2024, **220**, 119146.

[7] X. Xing, X. Zhang, Y. Feng and X. Yang, *J. Taiwan Inst. Chem. E.*, 2025, **166**, 105298.

[8] X. Hu, T. Zhang, B. Yang, M. Hao, Z. Chen, Y. Wei, Y. Liu, X. Wang and J. Yao, *Sep. Purif. Technol.*, 2024, **330**, 125367.

[9] M. Kloster, M.A. Mosiewicki and N.E. Marcovich, *Int. J. Biol. Macromol*., 2025, **329**, 147764.

[10] J. Wang, S. Sui, Y. Yang, Y. Lu, Y. Sheng, Y. Zhang and Z. Sun, *Sep. Purif. Technol*., 2025, **373**, 133429.

[11] Z. Zhang, J. Sun, X. Wei, G. Bai, W. Zhang, Y. Xiang, M. Li, J. Gao and X. Wang, *Int. J. Biol. Macromol*., 2025, **312**, 144188.

[12] Q. Zhang, Z. Wu and S. He, *Carbon*, 2025, **241**, 120384.